



**HAL**  
open science

## Population Pharmacokinetic Model of Plasma and Cellular Mycophenolic Acid in Kidney Transplant Patients from the CIMTRE Study

François Riglet, Julie Bertrand, Aurélie Barrail-Tran, Céline Verstuyft, Hugues Michelon, Henri Benech, Antoine Durrbach, Valérie Furlan, Caroline Barau

### ► To cite this version:

François Riglet, Julie Bertrand, Aurélie Barrail-Tran, Céline Verstuyft, Hugues Michelon, et al.. Population Pharmacokinetic Model of Plasma and Cellular Mycophenolic Acid in Kidney Transplant Patients from the CIMTRE Study. *Drugs in R&D*, 2020, 20 (4), pp.331-342. 10.1007/s40268-020-00319-y . hal-03209277

**HAL Id: hal-03209277**

**<https://hal.inrae.fr/hal-03209277>**

Submitted on 11 May 2021

**HAL** is a multi-disciplinary open access archive for the deposit and dissemination of scientific research documents, whether they are published or not. The documents may come from teaching and research institutions in France or abroad, or from public or private research centers.

L'archive ouverte pluridisciplinaire **HAL**, est destinée au dépôt et à la diffusion de documents scientifiques de niveau recherche, publiés ou non, émanant des établissements d'enseignement et de recherche français ou étrangers, des laboratoires publics ou privés.



# Population Pharmacokinetic Model of Plasma and Cellular Mycophenolic Acid in Kidney Transplant Patients from the CIMTRE Study

François Riglet<sup>1</sup> · Julie Bertrand<sup>1</sup> · Aurélie Barrail-Tran<sup>2,3,4</sup> · Céline Verstuylt<sup>5,6</sup> · Hugues Michelon<sup>2</sup> · Henri Benech<sup>7</sup> · Antoine Durrbach<sup>8,9</sup> · Valérie Furlan<sup>10</sup> · Caroline Barau<sup>11</sup>

Published online: 6 October 2020  
© The Author(s) 2020

## Abstract

**Background and Objective** Mycophenolate mofetil is widely used in kidney transplant recipients. Mycophenolate mofetil is hydrolysed by blood esterases to mycophenolic acid (MPA), the active drug. Although MPA therapeutic drug monitoring has been recommended to optimise the treatment efficacy by the area under the plasma concentration vs time curve, little is known regarding MPA concentrations in peripheral blood mononuclear cells, where MPA inhibits inosine monophosphate dehydrogenase. This study aimed to build a pharmacokinetic model using a population approach to describe MPA total and unbound concentrations in plasma and into peripheral blood mononuclear cells in 78 adult kidney transplant recipients receiving mycophenolate mofetil therapy combined with tacrolimus and prednisone.

**Methods** Total and unbound plasma concentrations and peripheral blood mononuclear cell concentrations were assayed. A three-compartment model, two for plasma MPA and one for peripheral blood mononuclear cell MPA, with a zero-order absorption and a first-order elimination was used to describe the data.

**Results** Mycophenolic acid average concentrations in peripheral blood mononuclear cells were well above half-maximal effective concentration for inosine monophosphate dehydrogenase and no relationship was found with the occurrence of graft rejection. Three covariates affected unbound and intracellular MPA pharmacokinetics: creatinine clearance, which has an effect on unbound MPA clearance, human serum albumin, which influences fraction unbound MPA and the *ABCB1* 3435 C>T (rs1045642) genetic polymorphism, which has an effect on MPA efflux transport from peripheral blood mononuclear cells.

**Conclusion** This population pharmacokinetic model demonstrated the intracellular accumulation of MPA, the efflux of MPA out of the cells being dependent on P-glycoprotein transporters. Nevertheless, further studies are warranted to investigate the relevance of MPA concentrations in peripheral blood mononuclear cells to dosing regimen optimisation.

## Key Points

This study highlights mycophenolic acid concentrations in peripheral blood mononuclear cells are well above the in vitro half maximal inhibitory concentration and the cellular kinetics is influenced by the *ABCB1* genetic polymorphism.

This model could be used to predict mycophenolic acid concentrations directly at its target site of action and to investigate the use of peripheral blood mononuclear cell mycophenolic acid exposure in a patient's follow-up after transplantation.

**Electronic supplementary material** The online version of this article (<https://doi.org/10.1007/s40268-020-00319-y>) contains supplementary material, which is available to authorized users.

✉ François Riglet  
francois.riglet@inserm.fr

Extended author information available on the last page of the article

## 1 Introduction

Mycophenolate mofetil (MMF) is the ester prodrug of mycophenolic acid (MPA) [1], an immunosuppressive drug used to prevent rejections in patients receiving renal allografts. Mycophenolic acid is a selective inhibitor of inosine-monophosphate dehydrogenase (IMPDH), an enzyme involved in the intracellular synthesis pathway of both T and B lymphocytes. Indeed, total plasma MPA concentrations above  $1 \text{ mg}\cdot\text{L}^{-1}$  are associated with an important decrease in lymphocyte proliferation ( $< 30\%$ ) [2].

The pharmacokinetics of MPA is characterised by a large inter- and intra-individual variability. For a fixed MMF dose, some studies described a ten-fold inter-patient variability in total plasma MPA exposure [3]. Some causes of this variability are well known such as body weight, concomitant immunosuppressive treatments, haemoglobin, human serum albumin (HSA) levels and creatinine clearance (CrCL) [4]. Polymorphisms of the genes coding for the UGT enzymes [5, 6] and uptake transporters [7, 8] have also been associated with total plasma MPA pharmacokinetic variability [9]. As an increasing number of people are successfully treated by organ transplantation, there is a consequent increase in the clinical use of MPA [10, 11] and the need for research on treatment optimisation. Prospective randomised studies demonstrated that therapeutic drug monitoring targeting total plasma MPA exposure (area under the concentration vs time curve from 0 to 12 h post-administration [ $\text{AUC}_{0-12\text{h}}$ ] between  $30$  and  $60 \text{ mg}\cdot\text{h}\cdot\text{L}^{-1}$ ) improved patient outcome [12–15], notably in the early post-transplantation period [16, 17]. According to results of Metz et al., despite therapeutic drug monitoring, the rejection rate in non-immunised renal transplant recipients is  $15.4\%$  in the first post-transplantation year [15]. These results question the use of total plasma MPA area under the concentration vs time curve as a predictor of target peripheral blood mononuclear cell (site of action) concentrations, and hence, the graft rejection risk.

Direct measurement of PBMC MPA concentrations may provide a better understanding of its immunosuppressive efficacy and distribution during graft rejection. Indeed, for cyclosporine and tacrolimus, lower PBMC concentrations, which were not reflected by whole blood concentrations, have been associated with significantly higher incidences of graft rejection [18, 19]. In fact, Thi et al. recently showed how concentrations of total plasma and PBMC MPA were correlated only in the first hours following the drug intake, but not with total plasma and PBMC MPA trough concentrations [20].

Two important factors of variation of these concentrations include (1) the binding of MPA to plasma albumin and (2) the role of PBMC uptake and efflux transporters, which can modulate intracellular concentrations. First, unbound MPA,

the active form, has high variability especially in the post-transplant period as MPA is strongly bound ( $\sim 97\%$ ) to HSA, which normalises within the post-transplantation period [12, 21]. Therefore, unbound MPA plasma exposure could be an interesting parameter to predict MPA concentrations at the intracellular site of action, rather than total MPA [22, 23]. Second, MPA entry into PBMCs depends on passive diffusion, active uptake and efflux transporters. P-glycoprotein (P-gp), encoded by the polymorphic *ABCB1* gene, is involved in the disposition of many drugs and expressed on PBMC membranes [24, 25] but so far no study has shown an association with MPA pharmacokinetics in humans. The MRP2 transporter, encoded by the *ABCC2* gene, is also expressed on the PBMC membrane, even if to a lesser extent [25] and the *ABCC2-24C>T* promoter polymorphism has been associated with an altered expression of MRP2 and a decrease of MPA hepatic efflux [26, 27].

The CIMTRE study collected plasma total and cellular MPA concentrations in kidney transplant patients receiving triple immunosuppressive therapy with a 6-month follow-up. The objective of the present work is to build a population pharmacokinetic (PK) model of these concentrations to explore the factors explaining the variability of MPA plasma and intracellular pharmacokinetics and its association with graft rejection.

## 2 Methods

### 2.1 CIMTRE Study

Between 2005 and 2008, patients followed in the Department of Nephrology of Bicêtre Hospital (Paris, France) were included in the study. They provided a written consent to be enrolled in the study and to undergo genotyping before their renal transplant. They received triple immunosuppressive therapy, including MMF (Cellcept<sup>®</sup>), tacrolimus (Prograf<sup>®</sup>) and prednisone (Cortancyl<sup>®</sup>). Mycophenolate mofetil was introduced with a fixed starting dose of  $1000 \text{ mg}$  twice daily and tacrolimus at a dose of  $0.2 \text{ mg}\cdot\text{kg}^{-1}$  per day. Tacrolimus dosages were adapted to reach a trough blood concentration range of  $5\text{--}15 \text{ ng}\cdot\text{mL}^{-1}$ . For MMF, dosage was adapted in the case of adverse effects. The Ethics Committee of CPP Ile de France VII approved the protocol of the CIMTRE study in June 2005.

During 6 months, five routine visits were performed for each patient: on the day of transplant (D0) and 15 days (D15), 1 month (M1), 2 months (M2) and 6 months after transplantation (M6). Age (years) and weight (kg) were collected at D0 whereas HSA ( $\text{g}\cdot\text{L}^{-1}$ ) and CrCL ( $\text{mL}\cdot\text{min}^{-1}$ ), calculated using the Cockcroft–Gault formula [28], were collected at each visit. The occurrence of graft rejection,

between two visits, was collected as a clinical marker of treatment efficacy.

Pharmacokinetic samples were collected at each visit. At D0, D15, M2 and M6, blood samples were drawn at pre-dose (before drug intake) and 30 min and 2 h after drug intake. At M1, samples were collected at pre-dose and 30 min, 1, 2, 4, 6 and 8 h after drug intake. Total plasma MPA concentrations ( $MPA_t$ ) were assayed on all samples. Unbound plasma ( $MPA_u$ ) and PBMC MPA concentrations ( $MPA_{cell}$ ) were assayed on pre-dose samples and 2 h after drug intake samples, at each visit. At M1, for 13 patients, unbound plasma and PBMC concentrations were also assayed at 4 and 6 h after drug intake samples.

## 2.2 Drug Assays

Total plasma concentrations were measured by reverse-phase high-performance liquid chromatography methods with ultraviolet detection. Similarly, unbound MPA was assayed in the ultrafiltrate after the centrifugation of plasma through Centrifree® devices (Millipore, Molsheim, France) by high-performance liquid chromatography with ultraviolet detection after direct injection of an ultrafiltrate into the chromatograph. The limit of quantitation of total plasma concentrations was  $0.1 \text{ mg.L}^{-1}$  and unbound plasma was  $0.01 \text{ mg.L}^{-1}$ . The PBMCs were isolated by centrifugation on a CPT® tube (Becton–Dickinson, Franklin Lake, NJ, USA). The PBMC concentration quantification was performed with a liquid chromatography-tandem mass spectrometry method [29]. The concentrations in PBMCs, expressed in ng per million cells, were converted to  $\text{mg.L}^{-1}$  using the average cell volume ( $0.2 \text{ pL}$ ) [30].

## 2.3 Genotyping

Genomic DNA was extracted from circulating blood leukocytes using the Puregene Kit (Gentra Systems, Minneapolis, MN, USA) according to the manufacturer's protocol and stored at  $-20 \text{ }^\circ\text{C}$ . For each patient, polymorphisms *ABCB1 3435C>T* (rs1045642), *ABCC2 24C>T* (rs717620) and *SLCO1B3 334T>G* (rs4149117) were genotyped. The genotyping was carried out using the TaqMan® allele discrimination assay (Applied Biosystems, Foster City, CA, USA) in duplicate, with separate experiments, to prevent genotyping errors. Allelic frequencies were calculated after counting genotypes and compared to allelic frequencies for other populations of the same ethnic group. Departure from the Hardy–Weinberg equilibrium was assessed by a  $\chi^2$  test ( $\alpha=5\%$ , 1 degree of freedom).

## 2.4 Pharmacokinetic Modelling

### 2.4.1 Structural Model

Based on a literature review, we did not test for a one-compartment distribution and used a two-compartment model to describe plasma unbound MPA ( $MPA_u$ ) distribution. We note  $V_{c_u}/F$  (L), the central compartment of volume,  $V_{p_u}/F$  (L), the peripheral compartment of volume and  $Q_u/F$  ( $\text{L.h}^{-1}$ ) the inter-compartmental clearance. We explored first- and zero-order absorption processes with rate constant,  $k_a$  ( $\text{h}^{-1}$ ) and  $Tk_0$  (h), with and without delay,  $Tlag$  (h) as well as simultaneous and sequential zero- and first-order absorption processes. Mycophenolic acid bioavailability,  $F$ , could not be estimated; therefore, clearances and volumes were apparent values (known up to the value of  $F$ ).

Graphic representation of unbound ( $MPA_u$ ) vs total ( $MPA_t$ ) observed MPA concentration showed a clear linear trend. Therefore, we decided not to explore a non-linear function to describe the protein binding, but a linear model as follows:

$$[MPA_t] = [MPA_u] + [MPA_b] = (1 + \theta_{pb}) \times [MPA_u], \quad (1)$$

where  $MPA_b$  represents the MPA bound to proteins and the parameter  $\theta_{pb}$  quantifies the ability of  $MPA_u$  to bind to proteins or the number of binding sites of  $MPA_u$  to HSA. The fraction of  $MPA_u$  is, therefore, expressed as [22, 31]:

$$f_u = \frac{[MPA_u]}{[MPA_t]} = \frac{[MPA_u]}{[MPA_u] + \theta_{pb} \times [MPA_u]} \quad (2)$$

$$= \frac{1}{1 + \theta_{pb}}.$$

Consequently, total MPA elimination first-order clearance  $CL_t/F$  was expressed as a function of  $MPA_u$  first-order clearance  $CL_u/F$  and  $\theta_{pb}$  as follows:

$$CL_t/F = \frac{CL_u/F}{1 + \theta_{pb}}. \quad (3)$$

To model the  $MPA_{cell}$ , we added a compartment of volume  $V_{cell}/F$  (L) with an input clearance from the central to the cell compartment,  $CL_{in}/F$  ( $\text{L.h}^{-1}$ ) and an output clearance from the cell to the central compartment,  $CL_{out}/F$  ( $\text{L.h}^{-1}$ ). To summarise,  $MPA_t$ ,  $MPA_u$  and  $MPA_{cell}$  concentrations were described by a three-compartment mammillary model.

## 2.5 Variability Model

The concentrations were analysed using a non-linear mixed-effects approach. The vector of PK individual parameters of

subject  $i$  at occasion  $k$ ,  $\phi_{ik}$  was defined using an exponential function to ensure positivity as follows:

$$\phi_{ik} = \mu \times e^{\eta_i} \times e^{\kappa_{ik}}, \quad (4)$$

where  $\mu$  is the vector of fixed effects,  $\eta_i \sim N(0, \Omega)$  is the vector of inter-individual random effects and  $\kappa_{ik} \sim N(0, \Gamma)$  is the vector of inter-occasion random effects.  $\Omega$  and  $\Gamma$  were the corresponding inter-individual variability and inter-occasion variability (IIV and IOV) matrixes. Given the number of model parameters,  $\Omega$  and  $\Gamma$  were supposed diagonal. Inter-occasion (or visit) variability actually captures the intra (or within)-patient variability.

Combined, proportional and constant variance models were investigated for the residual unexplained errors of MPA<sub>t</sub>, MPA<sub>u</sub> and MPA<sub>cell</sub>. Structural, residual unexplained variance (RUV), IIV and IOV model selection was based on the Bayesian Information Criterion (BIC). A BIC decrease of 2 points or less was not considered a strong enough signal and in that case the most parsimonious model was retained [32]. More specifically, starting with diagonal IIV and IOV matrixes, we used BIC in a stepwise backward process to remove all variances with a relative standard error (RSE) > 50%. We considered IIV and IOV independently, thus a parameter with no IIV (because removing IIV would not lead to a lower BIC) could have IOV (because estimating IOV would lead to a lower BIC).

## 2.6 Covariate Model

Based on physiological and clinical plausibility, we explored the following covariate associations on PK parameters with IIV; age and weight with all MPA<sub>u</sub> clearance and volume parameters, CrCL with CL<sub>u</sub>/F and Vp<sub>u</sub>/F, HSA with  $\theta_{pb}$ , and genetic polymorphisms with Vc<sub>u</sub>/F, CL<sub>u</sub>/F, CL<sub>out</sub>/F and V<sub>cell</sub>/F only if IIV were associated with these parameters. For each genetic polymorphism (wild and mutant allele, A and a), we evaluated three models: dominant (AA vs Aa plus aa), recessive (AA plus Aa vs aa) and additive (AA = 0, Aa = 1 and aa = 2).

First, a screening on empirical Bayesian estimates was performed at level 0.2. Of note, if no IOV could be estimated for CL<sub>u</sub>/F, Vp<sub>u</sub>/F or  $\theta_{pb}$ , we used the CrCL and HSA level at baseline. Second, after inclusion in the population model of all significant associations, a stepwise backward elimination was performed with Wald tests at level 0.05 to keep only the strongest association.

For continuous covariates, we used a multiplicative model:

$$\phi_{ikl} = \mu_l \times \left( \frac{\text{COV}_{ik}}{\text{COV}_{\text{REF}}} \right)^{\beta_{\mu_l, \text{COV}}} \times e^{\eta_{il}} \times e^{\kappa_{ikl}}, \quad (5)$$

where COV<sub>ik</sub> is the value of the covariate of interest of individual  $i$  at occasion  $k$  and  $\beta_{\mu_l, \text{COV}}$  is the effect size of its association with the  $l$ th PK parameter. Continuous covariates were centred on the study median or the reference value of 70 kg for weight (COV<sub>REF</sub>).

Categorical covariates were modelled as follows:

$$\phi_{ikl} = \mu_l \times \Pi_{\text{CAT}_{ik}}^{\beta_{\mu_l, \text{CAT}}} \times e^{\eta_{il}} \times e^{\kappa_{ikl}}, \quad (6)$$

where  $\Pi_{\text{CAT}_{ik}}$  is an indicator variable (=0 for the reference group and 1 for the comparator) for the covariate of interest of individual  $i$  at occasion  $k$  and  $\beta_{\mu_l, \text{CAT}}$  is the effect size of its association with the  $l$ th PK parameter.

## 2.7 Parameter Estimation and Model Evaluation

Estimations were carried out using the stochastic approximation expectation–maximisation algorithm. Relative standard errors and Log-likelihood were obtained using the linearisation approximation implemented in the software Monolix<sup>®</sup> version 2016 (Lixoft, Anthony, France). Internal validation was performed using basic and simulation-based goodness-of-fit plots [33].

## 2.8 Association Between Mycophenolic Acid Exposure and Graft Rejection

Individual area under the concentration vs time curves between 0 and 12 h post-administration (AUC<sub>0–12h</sub>) were predicted at D15, M1, M2 and M6 for MPA<sub>t</sub>, MPA<sub>u</sub> and MPA<sub>cell</sub> using empirical Bayesian estimates. Then, the ratios of cellular to unbound plasma MPA AUC<sub>0–12h</sub> were derived at D15, M1, M2 and M6.

A logistic regression was performed on the occurrence of graft rejection (at any visit) exploring the associations with HSA levels and CrCL at baseline, age and weight. Selection was performed using a stepwise forward selection at level 0.05. Using the final covariate model, we explored the relationship between plasma unbound and total AUC<sub>0–12h</sub> at D15 and PBMC AUC<sub>0–12h</sub> at D15 predicted by the population PK model and the occurrence of graft rejection.

Graphical and statistical analyses were performed using the open-source statistical software R version R-3.3.0.

## 3 Results

### 3.1 Characteristics of the Study Population

Eighty-two adult renal transplant recipients were enrolled in the CIMTRE study. Before the first visit, four patients were excluded because of serious adverse effects and/or left the

study. Demographic and genetic characteristics of the 78 patients included are summarised in Table 1. At inclusion, there were 45 (57%) men and the median [minimum–maximum] age was 50 [21–78] years. The distribution of genotypes for each single nucleotide polymorphism of uptake and efflux transporters did not significantly deviate from the Hardy–Weinberg equilibrium. Missing *ABCB1-3435C>T* and *ABCC2-24C>T* genotypes were imputed to the most common genotype in nine patients and *SLCO1B3-334T>G* genotypes in eight patients.

At each visit (i.e. D15, M1, M2 and M6), PK data were available for  $N=71, 73, 70$  and  $57$  patients, respectively. The sample size at the last visit decreased noticeably because some patients were excluded for haematological and digestive adverse effects. The evolution of CrCL and HSA levels is presented in Table 2. The median CrCL was  $54.81$  [ $40.55$ – $69.73$ ]  $\text{mL}\cdot\text{min}^{-1}$  and only 10% of the patients had a CrCL level below  $20 \text{ mL}\cdot\text{min}^{-1}$  at D15.

### 3.2 Pharmacokinetic Model Building

In total, 1931 concentration measurements, 925 for  $\text{MPA}_t$ , 560 for  $\text{MPA}_u$  and 446 for  $\text{MPA}_{\text{cell}}$  were analysed to build the population PK model with no measurement below the limit of quantitation. The 271 concentration–time curves (or point samples) of  $\text{MPA}_u$ ,  $\text{MPA}_t$  and  $\text{MPA}_{\text{cell}}$  from the patients in the CIMTRE study are displayed in Fig. 1.

#### 3.2.1 Base Model

A schematic of the structural model is given in Fig. 2. Visual exploration of  $\text{MPA}_t$  and  $\text{MPA}_u$  concentrations highlighted two elimination slopes, confirming our choice to not investigate a one-compartment model to describe MPA in plasma. For the absorption, a zero order best fitted the data compared with a first order ( $\Delta\text{BIC} = -3.34$ ). The fraction of unbound

$\text{MPA}_u$  was estimated at 1.8% (RSE = 3%). The  $\text{MPA}_{\text{cell}}$  concentrations were modelled with an additional compartment attached to the central compartment.

Proportional error models were selected for the RUV of  $\text{MPA}_t$ ,  $\text{MPA}_u$  and  $\text{MPA}_{\text{cell}}$  concentrations. Estimation of IOV led to a substantial reduction in the BIC ( $\Delta = -470$ ) and a reduction in RUV estimates; from 43 to 28% for  $\text{MPA}_t$ , from 46 to 28% for  $\text{MPA}_u$  and from 74 to 39% for  $\text{MPA}_{\text{cell}}$  (Table 3). It also led to a slight reduction in IIV; from 0.57 to 0.52 for  $\text{Tk}_0$  and from 0.87 to 0.77 for  $\text{CL}_{\text{out}}$ . Parameters  $Q_u/F$  and  $V_{\text{cell}}/F$  had IOV associated but no IIV, proving to be more subject to changes across occasions than across individuals in the population under study.

#### 3.2.2 Covariate Model

Univariate analyses of parameter-covariate associations are summarised in Table S1 of the Electronic Supplementary Material (ESM) and parameter estimates and their RSEs of the final covariate model are summarised in Table 3. Inter-individual variability and IOV shrinkage estimates for the base model are reported in Table S2 of the ESM.

In the final covariate model, CrCL was found to have an effect on  $\text{CL}_u/F$  with  $\text{CL}_u/F = 2465 \text{ L}\cdot\text{h}^{-1}$  for the patient with the highest CrCL ( $= 133.4 \text{ mL}\cdot\text{min}^{-1}$ ) and  $\text{CL}_u/F = 391 \text{ L}\cdot\text{h}^{-1}$  for the patient with the lowest CrCL ( $= 7.3 \text{ mL}\cdot\text{min}^{-1}$ ). Human serum albumin was found to influence  $f_u$ , with  $f_u = 1.3\%$  for an HSA of  $45.8 \text{ g}\cdot\text{L}^{-1}$  and  $f_u = 3.1\%$  for an HSA of  $24.7 \text{ g}\cdot\text{L}^{-1}$ . Finally, the *ABCB1 3435C>T* polymorphism was found to impact  $\text{CL}_{\text{out}}/F$ . The recessive model was the most significant. The *TT3425 ABCB1* homozygous patients were found associated with a lower  $\text{CL}_{\text{out}}/F$ ,  $36.6 \text{ L}\cdot\text{h}^{-1}$  vs  $58.5 \text{ L}\cdot\text{h}^{-1}$  in patient carriers of the genotype with the *C3435 ABCB1* allele.

**Table 1** Demographics, genotypes and clinical event occurrence of the 78 patients included in the CIMTRE study

Demographics	Median [minimum–maximum]
Age (years)	50.0 [21.0–78.0]
Weight (kg)	66.5 [36.0–125.0]
Genetic polymorphisms (genotypes)	Sample size (%)
<i>ABCB1 3435C&gt;T</i> (CC/CT/TT) <sup>a</sup>	30 (43.5)/28 (40.6)/11 (15.9)
<i>ABCC2 24C&gt;T</i> (CC/CT/TT) <sup>a</sup>	40 (58.0)/23 (33.3)/6 (8.7)
<i>SLCO1B3 334T&gt;G</i> (AA/AG/GG) <sup>b</sup>	50 (71.4)/17 (24.3)/3 (4.3)
Clinical event	Sample size (%)
Graft rejection (yes/no)	11 (14.1)/67 (85.9)

<sup>a</sup>Data missing for 9 patients, imputed to the most common genotype

<sup>b</sup>Data missing for 8 patients, imputed to the most common genotype

### 3.2.3 Model Evaluation

In Fig. 3, the prediction-corrected visual predictive plots for  $MPA_t$ ,  $MPA_u$  and  $MPA_{cell}$  demonstrated the adequacy of the final covariate model. Additional goodness-of-fit plots are provided in Figs. S1–3 of the ESM. Further, the condition number (i.e. the ratio of the maximal and minimal Eigen values of the estimation variance–covariance matrix) was equal to 13. We considered this value as reasonable in the context of a non-linear mixed-effect model. Moreover, parameters and their variability were provided with reasonable RSE (< 50%).

### 3.2.4 Mycophenolic Acid Exposure and Association with Graft Rejection

No link between HSA, CrCL, age, weight covariate at D0 and the occurrence of graft rejection was found. At D15, the median [minimum–maximum]  $AUC_{0-12h}$  was 47.9 [13.6–113.7]  $mg \cdot h \cdot L^{-1}$  for  $MPA_t$ , 0.9 [0.2–1.8]  $mg \cdot h \cdot L^{-1}$  for  $MPA_u$  and 27.30 [3.1–444.8]  $mg \cdot h \cdot L^{-1}$  for  $MPA_{cell}$  (Table 4). The median [minimum–maximum] ratio of cellular to unbound plasma MPA  $AUC_{0-12h}$  was 30.2 [3.0–585.0] at D15, 19.4 [1.8–256.3] at M1, 27.1 [4.2–305.3] at M2 and 26.8 [4.2–354.7] at M6, highlighting the important accumulation of MPA in cells in the first 15 days for a fixed dose of 200 mg once daily (96% of patients). No association between  $MPA_t$ ,  $MPA_u$  or  $MPA_{cell}$   $AUC_{0-12h}$  at D15 was found with the occurrence of graft rejection over the course of the CIMTRE study (Fig. S4 of the ESM).

**Table 2** Median [minimum–maximum] creatinine clearance (CrCL) and human serum albumin (HSA) level at each occasion (D15=15 days, M1=1 month, M2=2 months and M6=6 months after renal transplantation) with the corresponding sample size (*N*) in the CIMTRE study

	D15 ( <i>N</i> =71)	M1 ( <i>N</i> =73)	M2 ( <i>N</i> =70)	M6 ( <i>N</i> =57)
CrCL ( $mL \cdot min^{-1}$ )	47.4 [7.3–132.4]	54.6 [10.9–122.2]	59.0 [18.2–133.4]	60.7 [17.4–110.3]
HSA ( $g \cdot L^{-1}$ )	30.3 [20.4–43.6]	34.5 [21.8–43.1]	36.4 [21.7–63.1]	36.4 [23.7–48.5]

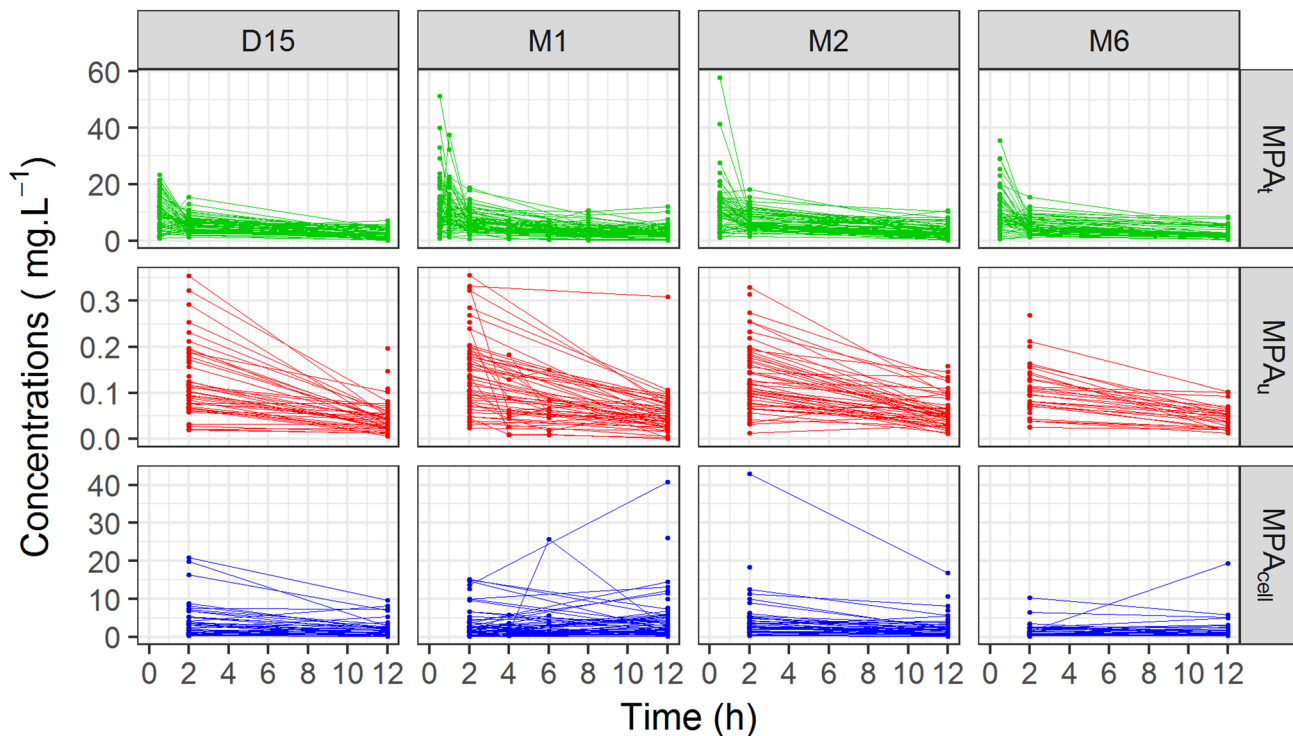


**Fig. 1** Individual concentrations ( $mg \cdot L^{-1}$ ) vs time (hours [h]) profiles for plasma total mycophenolic acid ( $MPA_t$ , top), plasma unbound mycophenolic acid ( $MPA_u$ , middle) and peripheral blood mononu-

clear cell mycophenolic acid ( $MPA_{cell}$ , bottom) at 15 days (D15), 1 month (M1), 2 months (M2) and 6 months (M6) after renal transplantation in the 78 patients from the CIMTRE study

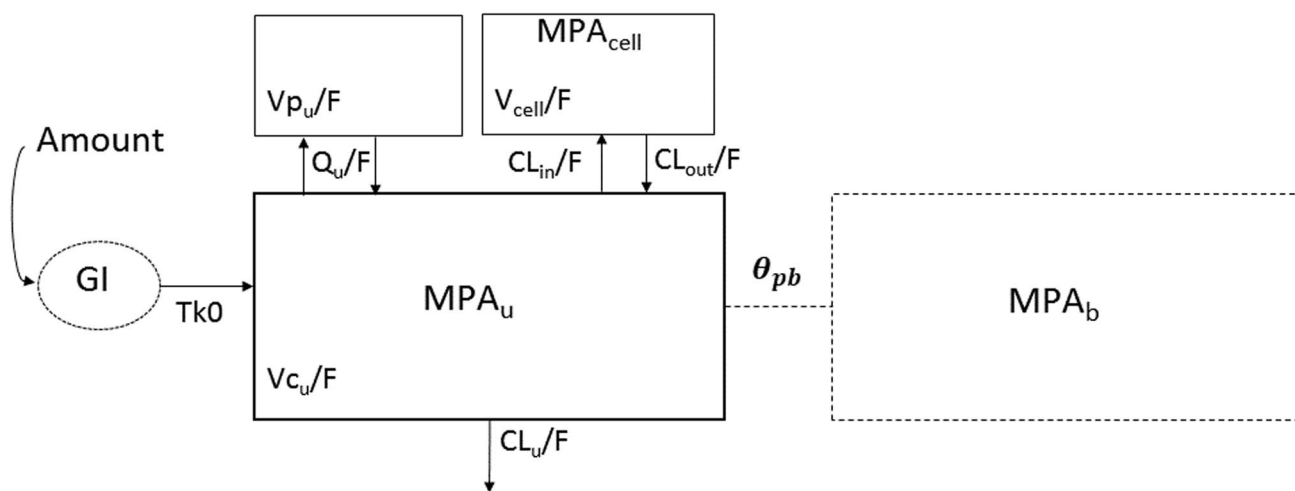


**Fig. 2** Schematic of the three-compartment model describing plasma total mycophenolic acid ( $MPA_t = (1 + \theta_{pb}) \times MPA_u$ ), plasma unbound mycophenolic acid ( $MPA_u$ ) and peripheral blood mononuclear cell mycophenolic acid ( $MPA_{cell}$ ). Parameters are  $Tk_0$ : the zero-order absorption constant from the gastrointestinal tract (GI),  $V_{c_u}/F$ : the apparent volume of the central compartment,  $V_{p_u}/F$ : the apparent volume of the peripheral compartment,  $Q_u/F$ : the intercompartmental

apparent clearance,  $CL_u/F$ : the elimination apparent clearance,  $V_{cell}/F$ : the apparent volume of the cellular compartment,  $CL_{in}/F$ : the apparent clearance of entrance into peripheral blood mononuclear cells and  $CL_{out}/F$ : the apparent clearance of exit from the peripheral blood mononuclear cells. The dashed compartment represents protein-bound mycophenolic acid ( $MPA_b = MPA_u \times \theta_{pb}$ ) with  $\theta_{pb}$ : the capacity of MPA to bind to proteins

## 4 Discussion

To our knowledge, this is the first PK model of plasma total, unbound and intracellular concentrations of MPA. This model quantifies the MPA accumulation in PBMCs as well as the influence of CrCL on MPA distribution and elimination, HSA level on MPA unbound fraction and the ABCB1 transporter on MPA efflux from the cells.

Mycophenolic acid plasma disposition in patients in the CIMTRE study was best described by a two-compartment model in agreement with the literature [34–36]. Similarly, the  $MPA_u$  fraction estimate (1.76%) was close to the value reported by Nowak and Shaw (1.8%  $\pm$  0.4%) [37]. Further, the  $CL_u/F$  estimate (15.65 L.h<sup>-1</sup>) was in the range of literature values (between 10 and 40 L.h<sup>-1</sup>) [4, 38] and the  $CL_u/F$  (900 L.h<sup>-1</sup>) estimate was close to the values reported by van Hest et al. and de Winter et al. (877 L.h<sup>-1</sup> and 747 L.h<sup>-1</sup>, respectively) [22, 35].

The influence of CrCL on  $CL_u/F$  had already been reported by van Hest et al. in 468 renal transplant patients [39] as well as the influence of HSA on MPA unbound fraction in 88 patients [22]. Although the later association led to a conflicting publication, [3, 12, 39] here, we chose not to test CrCL on the MPA unbound fraction. We believe the association found in the van Hest et al. article [39] is explained by  $MPA_u$  being cleared to a higher extent when CrCL increases, leading to a decrease of the unbound fraction and mechanically to an increase of  $\theta_{pb}$ . We found no influence of the genetic polymorphism on gene encoding for transporters MRP2 and OATP1B3 on MPA

pharmacokinetics. However, this is the first report of the association between the *ABCB1* 3435 C>T (rs1045642) polymorphism and MPA efflux from PBMCs. Although it was already shown that MPA is a substrate of P-gp in vitro [40] and in vivo using a mouse model [41], no other study reports this genetic association in humans. Interestingly, in *TT3435 ABCB1* homozygous patients,  $CL_{out}/F$  was lower than in *CC* and *CT3435 ABCB1* genotype patients. The efflux pump activity decreases and the MPA PBMC concentration was higher, even if plasma MPA pharmacokinetics has been largely investigated in relation to the *ABCC2* genotype, it was an interesting result. The *TT3435 ABCB1* genotype was previously described to lead to higher intracellular concentrations, most probably owing to lower P-gp activity towards the drug, as observed previously for cyclosporine A whole blood pharmacokinetics [42] but also for different substrates [43]. This *ABCB1* 3435C>T genetic single nucleotide polymorphism resulting in a silent mutation has probably been the most investigated so far. In accordance with such an effect at the protein level, the 3435C>T polymorphism has been associated with reduced messenger RNA expression and stability ex vivo [6], but this finding could not be confirmed in vitro [44]. More recently, this polymorphism has been associated with changes in substrate specificity [44].

Estimates for plasma total and unbound MPA  $AUC_{0-12h}$  were also close to literature values [31].  $MPA_{cell}$   $AUC_{0-12h}$  were higher than  $MPA_u$   $AUC_{0-12h}$  with elevated estimates for the ratio of cellular-to-unbound plasma MPA  $AUC_{0-12h}$ , implying an intracellular accumulation of MPA. Our model captured the accumulation with an input clearance into the



**Table 3** Estimates of fixed effects and coefficient of variations for the inter-individual variability and inter-occasion variability (IIV and IOV, %) of the base and covariate model parameters with associated

relative standard errors (RSEs, %) for patients included in the CIM-TRE study. Covariate coefficients (with associated RSE, %) are given below the corresponding model parameter

Parameters	Basic model			Covariate model		
	Fixed effects (RSE %)	IIV % (RSE %)	IOV % (RSE %)	Fixed effects (RSE %)	IIV % (RSE %)	IOV % (RSE %)
Tk0 (h)	1.29 (8)	45 (16)	66 (7)	1.29 (8)	44 (15)	60 (7)
$V_{c_u}/F$ (L)	1580 (11)	–	–	1620 (9)	–	–
$CL_{u_i}/F$ (L.h <sup>-1</sup> )	898 (5)	35 (10)	22 (9)	900 (4)	30 (11)	23 (9)
$\beta_{CL_{u_i}/F, CrCL}$	–	–	–	0.38 (19)	–	–
$Q_u/F$ (L.h <sup>-1</sup> )	2560 (13)	–	125 (11)	2040 (15)	–	153 (9)
$V_{p_u}/F$ (L)	16,900 (28)	173 (14)	111 (15)	19,400 (29)	70 (15)	89 (20)
$\beta_{V_{p_u}/F, CrCL}$	–	–	–	– 1.03 (40)	–	–
$\theta_{pb}$	55.3 (3)	23 (25)	–	56.5 (3)	16 (53)	–
$\beta_{\theta_{pb}, HSA}$	–	–	–	1.46 (15)	–	–
$CL_{in_i}/F$ (L.h <sup>-1</sup> )	1010 (13)	–	–	1200 (12)	–	–
$CL_{out_i}/F$ (L.h <sup>-1</sup> )	34.3 (16)	74 (11)	90 (6)	43.8 (16)	70 (12)	91 (6)
$\beta_{CL_{out_i}/F, ABCB1}$	–	–	–	–0.64 (44)	–	–
$V_{cell}/F$ (L)	1550 (20)	–	124 (13)	1980 (18)	–	33 (11)
$\sigma_u$ (%)	28 (6)	–	–	28 (6)	–	–
$\sigma_t$ (%)	29 (4)	–	–	29 (4)	–	–
$\sigma_{cell}$ (%)	39 (16)	–	–	39 (16)	–	–

$\beta_{CL_{out_i}/F, ABCB1}$  effect of *ABCB1* 3435 C>T genetic polymorphism on  $CL_{out_i}/F$ ,  $\beta_{CL_{u_i}/F, CrCL}$  effect of CrCL on  $CL_{u_i}/F$ ,  $\beta_{\theta_{pb}, HSA}$  effect of HAS on  $\theta_{pb}$ ,  $\beta_{V_{p_u}/F, CrCL}$  effect of CrCL on  $V_{p_u}/F$ ,  $\sigma_{cell}$  residual unexplained variability coefficient of variation for cellular MPA,  $\sigma_u$  residual unexplained variability coefficient of variation for plasma total MPA,  $\sigma_t$  residual unexplained variability coefficient of variation for plasma unbound MPA,  $CL_{in_i}/F$  apparent clearance of entrance into peripheral blood mononuclear cells,  $CL_{out_i}/F$  apparent clearance of exit from the peripheral blood mononuclear cells,  $CL_{u_i}/F$  elimination apparent clearance,  $\theta_{pb}$  capacity of MPA to bind to proteins,  $Q_u/F$  intercompartmental apparent clearance,  $Tk0$  zero-order absorption constant from the gastrointestinal track,  $V_{cell}/F$  apparent volume of the cellular compartment,  $V_{c_u}/F$  apparent volume of the central compartment,  $V_{p_u}/F$  apparent volume of the peripheral compartment

cell 30-fold superior to the output clearance from the cell. This result is consistent with the study of Thi et al., which highlighted an accumulation of MPA in PBMCs during the first 10 days after kidney transplantation, with  $MPA_{cell}$  concentrations following the plasma MPA concentrations variations in the early hours following the drug intake despite uncorrelated pre-dose concentrations [20]. These attenuated changes in PBMC exposures were characterised in our model by an input clearance into the cell 30-fold superior to the output clearance from the cell, resulting in an accumulation of MPA in PBMCs.

Despite a high IIV, plasma unbound and PBMC MPA  $AUC_{0-12h}$  varied only slightly between occasions over the 6-month post-transplantation period. These parameters could therefore be more reliable than total plasma concentrations suggested by some authors for therapeutic drug monitoring [13]. Similarly, our estimates for plasma total and unbound MPA  $AUC_{0-12h}$  were close to literature values [31]. Further, the minimal average concentration (which was obtained using area under the concentration vs time curve during the interval dosing divided by the interval dosing, i.e.  $AUC_{0-12h}/12$ ) of cellular MPA concentrations at each visit was well above 0.06 mg L<sup>-1</sup>, the half-maximal effective

concentration for IMPDH estimated by Li et al. In fact, Sugiyama et al. studied half maximal inhibitory concentration effective MPA concentrations for IMPDH in PBMCs in vitro and obtained an even lower half maximal inhibitory concentration of 0.0079 mg.L<sup>-1</sup>, a value significantly lower than  $MPA_{cell}$  concentrations derived from our model [45].

This study has some limitations. First, some parameters conserved large inter- and intra-individual variabilities, notably the apparent exit clearance from the cell. This could partly result from the complex isolation procedure and the difficult automation of the MPA dosing method in PBMCs. Additionally, we approximated the PBMC volume arbitrarily to 0.2 pL [30], whereas this mean volume is known to vary between PBMC cell types. Further, this approximation can distort PBMC concentrations [46] and complicates comparisons with studies reporting PBMC concentrations in ng.10<sup>6</sup> cells<sup>-1</sup>. The large variabilities remaining on the peripheral apparent clearance and volume as well as on the absorption parameter probably result from the sparseness of the sampling design, which also prevented the observation, and the modelling, of a double peak due to the MPA enterohepatic recirculation [31, 35, 47].

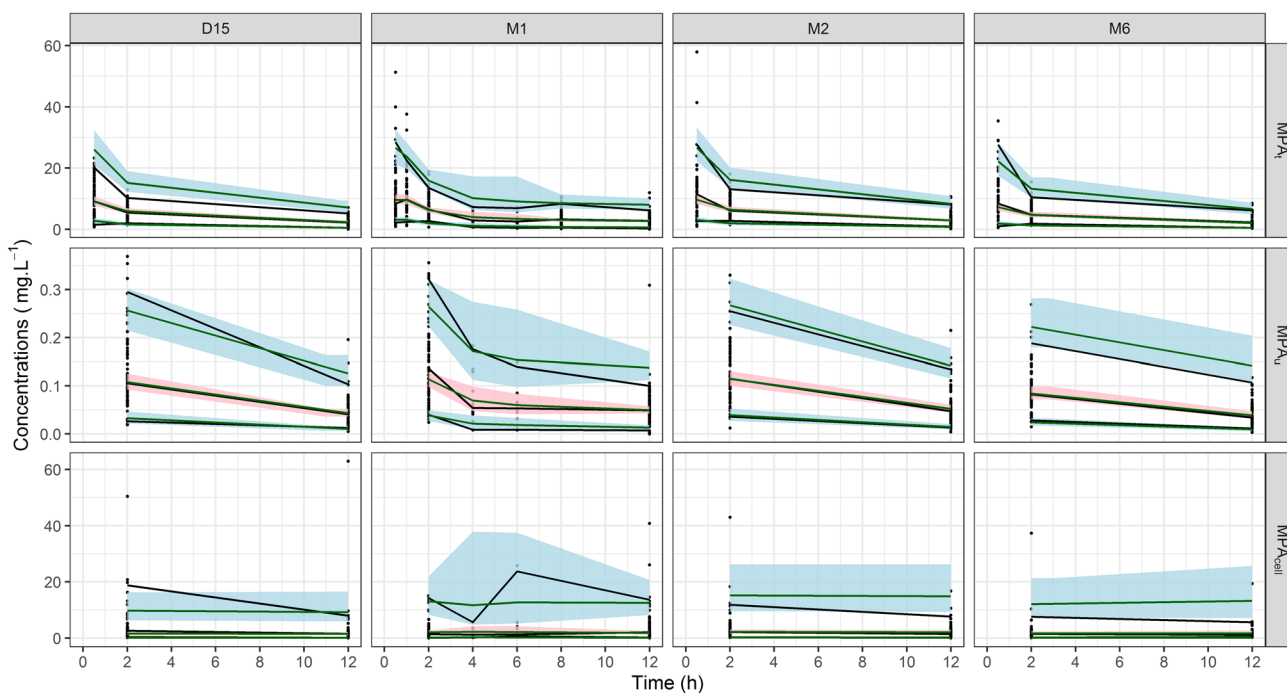


**Fig. 3** Prediction-corrected visual predictive check plots for plasma total mycophenolic acid ( $MPA_t$ , top), plasma unbound mycophenolic acid ( $MPA_u$ , middle) and peripheral blood mononuclear cell mycophenolic acid ( $MPA_{cell}$ , bottom) based on 500 simulated datasets using the final covariate model. The black lines represent the 5th, 50th and 95th percentiles of the model predictions and the green lines

represent the 5th, 50th and 95th percentiles of the observations. The blue and pink areas represent the 90% confidence intervals around the fifth (bottom), 50th (middle) and 95th (top) model-predicted percentiles. The blue dots represent observations from the 78 patients in the CIMTRE study

**Table 4** Median [minimum–maximum] area under the concentration vs time curve from 0 to 12 h post-administration for total and unbound plasma mycophenolic acid (MPA) and cellular MPA ( $MPA_t$ ,

$MPA_u$  and  $MPA_{cell}$ ) at each occasion (D15=15 days, M1=1 month, M2=2 months and M6=6 months after renal transplantation) with the corresponding sample size ( $N$ ) in the CIMTRE study

	D15 ( $N=71$ )	M1 ( $N=73$ )	M2 ( $N=70$ )	M6 ( $N=57$ )
$MPA_t$ (mg.h.L <sup>-1</sup> )	47.9 [13.6–113.7]	48.9 [10.4–124.7]	54.6 [12.9–121.5]	40.2 [6.7–81.7]
$MPA_u$ (mg.h.L <sup>-1</sup> )	0.9 [0.2–1.8]	0.9 [0.3–2.8]	1.0 [0.4–1.8]	0.7 [0.2–1.4]
$MPA_{cell}$ (mg.h.L <sup>-1</sup> )	27.33 [3.1–444.8]	19.7 [1.5–191.0]	24.2 [3.4–407.2]	18.9 [2.7–319.9]

Another limitation with regard to the inter- and intra-individual variability is the choice of exploring diagonal matrices only. Finally, in the CIMTRE study, patients received MMF concomitantly with tacrolimus and prednisone, which also influences the incidence of acute rejection, estimated at 14.1% with most graft rejections occurring before D15. With this incidence rate out of 78 patients, we would have had a power of 80% to detect a 50% drop in PBMC AUC<sub>0–12h</sub> of cases if the IIV has been three times lower. The high IIV, the elevated MPA concentrations in the upper range of the consensus report [48], and the low number and early occurrence of clinical events hindered the quantification of

the link between plasma and cellular MPA kinetics and the occurrence of graft rejection.

### 5 Conclusions

To conclude, this model can be used to compute individual MPA exposure at the site of action but further studies are warranted to explore the relationship between these exposures and clinical events such as graft rejection and to investigate whether unbound MPA concentrations or MPA concentration in PBMCs could be relevant parameters to optimise dosing regimens.

**Acknowledgements** The authors thank all the contributors of the CIM-TRE study: the Department of Nephrology of Bicêtre Hospital, Dr. Anne-Marie Taburet, Caroline Bazzoli, Dr. Laurent Becquemont and Alexia Letierce.

## Declarations

**Funding** This work was supported by a grant from the Hospital Clinical Research Program of the French Ministry of Health. The funders had no role in the study design, data collection and analysis, decision to publish or preparation of the manuscript.

**Conflicts of interest/competing interests** François Riglet, Julie Bertrand, Aurélie Barrail-Tran, Céline Verstuyft, Hugues Michelon, Henri Benech, Antoine Durrbach, Valérie Furlan and Caroline Barau have no conflicts of interest that are directly relevant to the content of this article.

**Ethics approval** All procedures performed in studies involving human participants were in accordance with the ethical standards of the institutional and/or national research committee and with the 1964 Helsinki Declaration and its later amendments or comparable ethical standards.

**Consent to participate** Informed consent was obtained from all individual participants included in the study.

**Consent for publication** Patients signed informed consent regarding publishing their data.

**Availability of data and material** The data supporting the findings of this study are available on request to the corresponding author. The data are not publicly available because of privacy or ethical restrictions.

**Code availability** Monolix codes are available upon request to the corresponding author.

**Authors' contributions** AD and VF designed the research. CB, ABT and VF performed the assays of plasma MPA concentrations and participated in the clinical and pharmacokinetic interpretation of the study. HB performed the assay of the cellular MPA concentrations. CV carried out the genotyping. FR analysed the data and performed the pharmacokinetic modelling under the supervision of JB. All authors participated in writing the manuscript.

**Open Access** This article is licensed under a Creative Commons Attribution-NonCommercial 4.0 International License, which permits any non-commercial use, sharing, adaptation, distribution and reproduction in any medium or format, as long as you give appropriate credit to the original author(s) and the source, provide a link to the Creative Commons licence, and indicate if changes were made. The images or other third party material in this article are included in the article's Creative Commons licence, unless indicated otherwise in a credit line to the material. If material is not included in the article's Creative Commons licence and your intended use is not permitted by statutory regulation or exceeds the permitted use, you will need to obtain permission directly from the copyright holder. To view a copy of this licence, visit <http://creativecommons.org/licenses/by-nc/4.0/>.


## References

- Halloran P, Mathew T, Tomlanovich S, Groth C, Hooftman L, Barker C. Mycophenolate mofetil in renal allograft recipients: a pooled efficacy analysis of three randomized, double-blind, clinical studies in prevention of rejection: the International Mycophenolate Mofetil Renal Transplant Study Groups. *Transplantation*. 1997;63(1):39–47.
- Brunet M, Cirera I, Martorell J, et al. Sequential determination of pharmacokinetics and pharmacodynamics of mycophenolic acid in liver transplant patients treated with mycophenolate mofetil. *Transplantation*. 2006;81(4):541–6. <https://doi.org/10.1097/01.tp.0000200307.79962.48>.
- van Hest RM, Mathot RAA, Pescovitz MD, Gordon R, Mamelok RD, van Gelder T. Explaining variability in mycophenolic acid exposure to optimize mycophenolate mofetil dosing: a population pharmacokinetic meta-analysis of mycophenolic acid in renal transplant recipients. *J Am Soc Nephrol*. 2006;17(3):871–80. <https://doi.org/10.1681/ASN.2005101070>.
- Kiang TKL, Ensom MHH. Population pharmacokinetics of mycophenolic acid: an update. *Clin Pharmacokinetics*. 2018;57(5):547–58. <https://doi.org/10.1007/s40262-017-0593-6>.
- Bernard O, Guillemette C. The main role of UGT1A9 in the hepatic metabolism of mycophenolic acid and the effects of naturally occurring variants. *Drug Metab Dispos Biol Fate Chem*. 2004;32(8):775–8.
- Picard N, Ratanasavanh D, Prémaud A, Le Meur Y, Marquet P. Identification of the UDP-glucuronosyltransferase isoforms involved in mycophenolic acid phase II metabolism. *Drug Metab Dispos Biol Fate Chem*. 2005;33(1):139–46. <https://doi.org/10.1124/dmd.104.001651>.
- Picard N, Yee SW, Woillard JB, et al. The role of organic anion-transporting polypeptides and their common genetic variants in mycophenolic acid pharmacokinetics. *Clin Pharmacol Ther*. 2010;87(1):100–8. <https://doi.org/10.1038/clpt.2009.205>.
- Kagaya H, Niioka T, Saito M, et al. Effect of hepatic drug transporter polymorphisms on the pharmacokinetics of mycophenolic acid in patients with severe renal dysfunction before renal transplantation. *Xenobiotica Fate Foreign Compd Biol Syst*. 2017;47(10):916–22. <https://doi.org/10.1080/00498254.2016.1235742>.
- Michelon H, König J, Durrbach A, et al. SLC01B1 genetic polymorphism influences mycophenolic acid tolerance in renal transplant recipients. *Pharmacogenomics*. 2010;11(12):1703–13. <https://doi.org/10.2217/pgs.10.132>.
- Stegall MD, Somerville KT, Everly MJ, et al. The importance of drug safety and tolerability in the development of new immunosuppressive therapy for transplant recipients: the Transplant Therapeutics Consortium's position statement. *Am J Transplant*. 2019;19(3):625–32. <https://doi.org/10.1111/ajt.15214>.
- Gardiner KM, Tett SE, Staatz CE. Multinational evaluation of mycophenolic acid, tacrolimus, cyclosporin, sirolimus, and everolimus utilization. *Ann Transplant*. 2016;21:1–11. <https://doi.org/10.12659/aot.895664>.
- van Gelder T, Shaw LM. The rationale for and limitations of therapeutic drug monitoring for mycophenolate mofetil in transplantation. *Transplantation*. 2005;80(2 Suppl.):S244–53. <https://doi.org/10.1097/01.tp.0000186380.61251.fc>.
- Kuypers DRJ, Meur YL, Cantarovich M, et al. Consensus report on therapeutic drug monitoring of mycophenolic acid in solid organ transplantation. *Clin J Am Soc Nephrol*. 2010;5(2):341–58. <https://doi.org/10.2215/CJN.07111009>.
- Tett SE, Saint-Marcoux F, Staatz CE, et al. Mycophenolate, clinical pharmacokinetics, formulations, and methods for assessing

- drug exposure. *Transplant Rev.* 2011;25(2):47–57. <https://doi.org/10.1016/j.trre.2010.06.001>.
15. Metz DK, Holford N, Kausman JY, et al. Optimizing mycophenolic acid exposure in kidney transplant recipients: time for target concentration intervention. *Transplantation.* 2019;103(10):2012–30. <https://doi.org/10.1097/TP.0000000000002762>.
  16. Le Meur Y, Borrows R, Pescovitz MD, et al. Therapeutic drug monitoring of mycophenolates in kidney transplantation: report of The Transplantation Society consensus meeting. *Transplant Rev (Orlando).* 2011;25(2):58–64. <https://doi.org/10.1016/j.trre.2011.01.002>.
  17. Hale MD, Nicholls AJ, Bullingham RES, et al. The pharmacokinetic-pharmacodynamic relationship for mycophenolate mofetil in renal transplantation. *Clin Pharmacol Ther.* 1998;64(6):672–83. [https://doi.org/10.1016/S0009-9236\(98\)90058-3](https://doi.org/10.1016/S0009-9236(98)90058-3).
  18. Falck P, Åsberg A, Guldseth H, et al. Declining intracellular T-lymphocyte concentration of cyclosporine A precedes acute rejection in kidney transplant recipients. *Transplantation.* 2008;85(2):179–84. <https://doi.org/10.1097/TP.0b013e31815feede>.
  19. Capron A, Lerut J, Latinne D, Rahier J, Haufroid V, Wallemacq P. Correlation of tacrolimus levels in peripheral blood mononuclear cells with histological staging of rejection after liver transplantation: preliminary results of a prospective study. *Transpl Int.* 2012;25(1):41–7. <https://doi.org/10.1111/j.1432-2277.2011.01365.x>.
  20. Thi MT, Mourad M, Capron A, Musuamba Tshinanu F, Vincent M-F, Wallemacq P. Plasma and intracellular pharmacokinetic-pharmacodynamic analysis of mycophenolic acid in de novo kidney transplant patients. *Clin Biochem.* 2015;48(6):401–5. <https://doi.org/10.1016/j.clinbiochem.2014.12.005>.
  21. Bullingham RES, Nicholls AJ, Kamm BR. Clinical pharmacokinetics of mycophenolate mofetil. *Clin Pharmacokinet.* 1998;34(6):429–55. <https://doi.org/10.2165/00003088-199834060-00002>.
  22. van Hest RM, van Gelder T, Vulto AG, Shaw LM, Mathot RAA. Pharmacokinetic modelling of the plasma protein binding of mycophenolic acid in renal transplant recipients. *Clin Pharmacokinet.* 2009;48(7):463–76. <https://doi.org/10.2165/11312600-000000000-00000>.
  23. Atcheson BA, Taylor PJ, Mudge DW, et al. Mycophenolic acid pharmacokinetics and related outcomes early after renal transplant. *Br J Clin Pharmacol.* 2005;59(3):271–80. <https://doi.org/10.1111/j.1365-2125.2004.02235.x>.
  24. Ansermot N, Rebsamen M, Chabert J, et al. Influence of ABCB1 gene polymorphisms and P-glycoprotein activity on cyclosporine pharmacokinetics in peripheral blood mononuclear cells in healthy volunteers. *Drug Metab Lett.* 2008;2(2):76–82.
  25. Giraud C, Manceau S, Treluyer J-M. ABC transporters in human lymphocytes: expression, activity and role, modulating factors and consequences for antiretroviral therapies. *Expert Opin Drug Metab Toxicol.* 2010;6(5):571–89. <https://doi.org/10.1517/17425251003601953>.
  26. Kock K, Brouwer KL. A perspective on efflux transport proteins in the liver. *Clin Pharmacol Ther.* 2012;92(5):599–612. <https://doi.org/10.1038/clpt.2012.79>.
  27. Li L-Q, Chen D-N, Li C-J, et al. Impact of UGT2B7 and ABC22 genetic polymorphisms on mycophenolic acid metabolism in Chinese renal transplant recipients. *Pharmacogenomics.* 2018;19(17):1323–34. <https://doi.org/10.2217/pgs-2018-0114>.
  28. Cockcroft DW, Gault MH. Prediction of creatinine clearance from serum creatinine. *Nephron.* 1976;16(1):31–41.
  29. Bénech H, Hascoët S, Furlan V, Pruvost A, Durrbach A. Development and validation of an LC/MS/MS assay for mycophenolic acid in human peripheral blood mononuclear cells. *J Chromatogr B Analyt Technol Biomed Life Sci.* 2007;853(1–2):168–74. <https://doi.org/10.1016/j.jchromb.2007.03.008>.
  30. Segel GB, Cokelet GR, Lichtman MA. The measurement of lymphocyte volume: importance of reference particle deformability and counting solution tonicity. *Blood.* 1981;57(5):894–9.
  31. Colom H, Andreu F, van Gelder T, et al. Prediction of free from total mycophenolic acid concentrations in stable renal transplant patients: a population-based approach. *Clin Pharmacokinet.* 2018;57(7):877–93. <https://doi.org/10.1007/s40262-017-0603-8>.
  32. Raftery AE. Bayes factors and BIC: comment on “A Critique of the Bayesian Information Criterion for Model Selection”. *Sociol Methods Res.* 1999;27(3):411–27. <https://doi.org/10.1177/0049124199027003005>.
  33. Bergstrand M, Hooker AC, Wallin JE, Karlsson MO. Prediction-corrected visual predictive checks for diagnosing nonlinear mixed-effects models. *AAPS J.* 2011;13(2):143–51. <https://doi.org/10.1208/s12248-011-9255-z>.
  34. van Hest RM, van Gelder T, Vulto AG, Mathot RAA. Population pharmacokinetics of mycophenolic acid in renal transplant recipients. *Clin Pharmacokinet.* 2005;44(10):1083–96. <https://doi.org/10.2165/00003088-200544100-00006>.
  35. de Winter BCM, van Gelder T, Sombogaard F, Shaw LM, van Hest RM, Mathot RAA. Pharmacokinetic role of protein binding of mycophenolic acid and its glucuronide metabolite in renal transplant recipients. *J Pharmacokinet Pharmacodyn.* 2009;36(6):541–64. <https://doi.org/10.1007/s10928-009-9136-6>.
  36. Li H, Mager DE, Bemer MJ, et al. A limited sampling schedule to estimate mycophenolic acid area under the concentration-time curve in hematopoietic cell transplantation recipients. *J Clin Pharmacol.* 2012;52(11):1654–64. <https://doi.org/10.1177/0091270011429567>.
  37. Nowak I, Shaw LM. Mycophenolic acid binding to human serum albumin: characterization and relation to pharmacodynamics. *Clin Chem.* 1995;41(7):1011–7.
  38. Sherwin CMT, Fukuda T, Brunner HI, Goebel J, Vinks AA. The evolution of population pharmacokinetic models to describe the enterohepatic recycling of mycophenolic acid in solid organ transplantation and autoimmune disease. *Clin Pharmacokinet.* 2011;50(1):1–24. <https://doi.org/10.2165/11536640-000000000-00000>.
  39. van Hest RM, van Gelder T, Bouw R, et al. Time-dependent clearance of mycophenolic acid in renal transplant recipients. *Br J Clin Pharmacol.* 2007;63(6):741–52. <https://doi.org/10.1111/j.1365-2125.2006.02841.x>.
  40. Sawamoto T, van Gelder T, Christians U, Okamura N, Jacobsen W, Benet L. Membrane transport of mycophenolate mofetil and its active metabolite, mycophenolic acid in MDCK and MDR1-MDCK cell monolayers. *J Heart Lung Transplant.* 2001;20(2):234–5.
  41. Wang J, Figurski M, Shaw LM, Burckart GJ. The impact of P-glycoprotein and Mrp2 on mycophenolic acid levels in mice. *Transpl Immunol.* 2008;19(3–4):192–6. <https://doi.org/10.1016/j.trim.2008.05.009>.
  42. Crettol S, Venetz J-P, Fontana M, et al. Influence of ABCB1 genetic polymorphisms on cyclosporine intracellular concentration in transplant recipients. *Pharmacogenet Genom.* 2008;18(4):307–15. <https://doi.org/10.1097/FPC.0b013e3182f7046f>.
  43. Haufroid V. Genetic polymorphisms of ATP-binding cassette transporters ABCB1 and ABC22 and their impact on drug disposition. *Curr Drug Targ.* 2011;12(5):631–46. <https://doi.org/10.2174/138945011795378487>.
  44. Kimchi-Sarfaty C, Oh JM, Kim I-W, et al. A “silent” polymorphism in the MDR1 gene changes substrate specificity. *Science.* 2007;315(5811):525–8. <https://doi.org/10.1126/science.1135308>.

45. Sugiyama K, Isogai K, Toyama A, et al. Pharmacodynamic parameters of immunosuppressive drugs are not correlated with age, duration of dialysis, percentage of lymphocytes or lymphocyte stimulation index in renal transplant recipients. *Biol Pharm Bull.* 2008;31(11):2146–9. <https://doi.org/10.1248/bpb.31.2146>.
46. Bazzoli C, Jullien V, Tiec CL, Rey E, Mentré F, Taburet A-M. Intracellular pharmacokinetics of antiretroviral drugs in HIV-infected patients, and their correlation with drug action. *Clin Pharmacokinet.* 2010;49(1):17–45. <https://doi.org/10.2165/11318110-000000000-00000>.
47. Sherwin CMT, Sagcal-Gironella ACP, Fukuda T, Brunner HI, Vinks AA. Development of population PK model with enterohepatic circulation for mycophenolic acid in patients with childhood-onset systemic lupus erythematosus. *Br J Clin Pharmacol.* 2012;73(5):727–40. <https://doi.org/10.1111/j.1365-2125.2011.04140.x>.
48. Cantarovich M, Brown NW, Ensom MHH, et al. Mycophenolate monitoring in liver, thoracic, pancreas, and small bowel transplantation: a consensus report. *Transpl Rev.* 2011;25(2):65–77. <https://doi.org/10.1016/j.trre.2010.12.001>.

## Affiliations

François Riglet<sup>1</sup>  · Julie Bertrand<sup>1</sup> · Aurélie Barrail-Tran<sup>2,3,4</sup> · Céline Verstuylft<sup>5,6</sup> · Hugues Michelon<sup>2</sup> · Henri Benech<sup>7</sup> · Antoine Durrbach<sup>8,9</sup> · Valérie Furlan<sup>10</sup> · Caroline Barau<sup>11</sup>

<sup>1</sup> Université de Paris, INSERM, IAME, 75018 Paris, France

<sup>2</sup> AP-HP, Université Paris-Saclay, Hôpital Bicêtre, Service de Pharmacie Clinique, Le Kremlin-Bicêtre, France

<sup>3</sup> Université Paris-Saclay, INSERM, CEA, Centre de recherche en Immunologie des infections virales et des maladies auto-immunes, 92265 Fontenay-aux-Roses, France

<sup>4</sup> Faculté de Pharmacie, Université Paris-Saclay, Châtenay-Malabry, France

<sup>5</sup> AP-HP, Hôpital Bicêtre, Service de Génétique Moléculaire, Pharmacogénétique et Hormonologie, Le Kremlin-Bicêtre, France

<sup>6</sup> Université Paris-Saclay, INSERM, CESP, MOODS Team, Faculté de Médecine, 94270 Le Kremlin Bicêtre, France

<sup>7</sup> Département Médicaments et technologies pour la santé, Université Paris-Saclay, CEA, INRAE, Gif-sur-Yvette, France

<sup>8</sup> AP-HP, Hôpital Henri Mondor, Service de Néphrologie, Créteil, France

<sup>9</sup> Université Paris-Saclay, INSERM, UMR 1137, Orsay, France

<sup>10</sup> AP-HP, Hôpitaux Universitaires Paris-Sud, Hôpital Bicêtre, Laboratoire de Pharmacologie Toxicologie, Le Kremlin-Bicêtre, France

<sup>11</sup> AP-HP, Hôpital Henri Mondor, Plateforme de Ressources Biologiques, Créteil, France